

Received 7 November 2018

Accepted 15 November 2018

Edited by A. J. Lough, University of Toronto,
Canada

Keywords: crystal structure; triazole; pyrimidine; hydrogen bond; π - π -stacking; Hirshfeld surface analysis.

CCDC reference: 1879279

Supporting information: this article has supporting information at journals.iucr.org/e

Crystal structure and Hirshfeld surface analysis of 5-methyl-1,2,4-triazolo[1,5-*a*]pyrimidine

Sanae Lahmidi,^{a,*} Nada Kheira Sebbar,^b Tuncer Hökelek,^c Karim Chkirate,^a Joel T. Mague^d and El Mokhtar Essassi^a

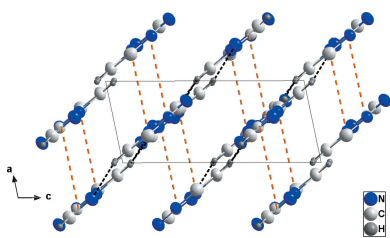
^aLaboratoire de Chimie Organique Hétérocyclique URAC 21, Pôle de Compétence Pharmacochimie, Av. Ibn Battouta, BP 1014, Faculté des Sciences, Université Mohammed V, Rabat, Morocco, ^bLaboratoire de Chimie Bioorganique Appliquée, Faculté des Sciences, Université Ibn Zohr, Agadir, Morocco, ^cDepartment of Physics, Hacettepe University, 06800 Beytepe, Ankara, Turkey, and ^dDepartment of Chemistry, Tulane University, New Orleans, LA 70118, USA.

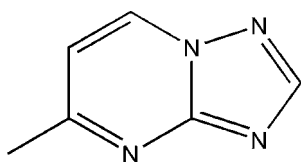
*Correspondence e-mail: sanaelahmidi2018@gmail.com

The nine-membered ring system of the title compound, C₆H₆N₄, is essentially planar. In the crystal, molecules are linked *via* C—H_{Trz}···N_{Trz} and C—H_{Pyrm}···N_{Trz} (Trz = triazole and Pyrm = pyrimidine) hydrogen bonds together with weaker C—H_{Pyrm}···N_{Pyrm} hydrogen bonds to form layers parallel to (102). The layers are further connected by π - π -stacking interactions between the nine-membered ring system [centroid-centroid = 3.7910 (8) Å], forming oblique stacks along the *a*-axis direction. The Hirshfeld surface analysis of the crystal structure indicates that the most important contributions for the crystal packing are from H···N/N···H (40.1%), H···H (35.3%), H···C/C···H (9.5%), N···C/C···N (9.0%), N···N (3.1%) and C···C (3.0%) interactions and that hydrogen-bonding and van der Waals interactions are the dominant interactions in the crystal packing. No significant C—H··· π interactions are observed.

1. Chemical context

In recent years, much attention has been paid to the development of new methods for the synthesis and investigation of biological and pharmacological properties of [1,2,4]triazolo[1,5-*a*]pyrimidine derivatives (Chebanov *et al.*, 2010; Lahmidi *et al.*, 2016*a,b*, 2018; Sedash *et al.*, 2012). Thus, these compounds have also received successful applications for the preparation of new poly-condensed heterocycles (Beck *et al.*, 2011). Among the various classes of nitrogen-containing heterocyclic compounds such as triazolopyrimidine derivatives display a broad spectrum of biological activities, including anti-inflammatory (Ashour *et al.*, 2013), anticancer (Hoffmann *et al.*, 2017) and antibacterial (Mabkhot *et al.*, 2016) activities. In a continuation of our research on the elaboration of new methods for the synthesis of various heterocyclic systems, we investigated the reaction of bis(2-chloroethyl)amine hydrochloride with ethyl 2-(5-methyl-1,2,4-triazolo[1,5-*a*]pyrimidin-7-yl)acetate under phase-transfer catalysis conditions using tetra-*n*-butyl ammonium-bromide (TBAB) as catalyst and potassium carbonate as base to afford the title compound, 5-methyl-1,2,4-triazolo[1,5-*a*]pyrimidine, (I). We report herein its molecular and crystal structures along with the results of a Hirshfeld surface analysis.





2. Structural commentary

In the title compound (Fig. 1), the nine-membered ring is planar to within 0.004 (1) Å (for atom C5), and the r.m.s. deviation of the fitted atoms is 0.009 Å. Methyl atom C6 is displaced by 0.032 (1) Å from the ring system.

3. Supramolecular features

In the crystal, C–H_{Trz}⋯N_{Trz} and C–H_{Pyrm}⋯N_{Trz} (Trz = triazole and Pyrm = pyrimidine) hydrogen bonds (Table 1), together with weaker C–H_{Pyrm}⋯N_{Pyrm} hydrogen bonds, link the molecules, forming layers parallel to (1̄02) (Fig. 2). The layers are further connected by π–π-stacking interactions between the nine-membered rings [centroid–centroid distance = 3.7910 (8) Å], forming oblique stacks along the *a*-axis direction (Fig. 3). No significant C–H⋯π interactions are observed.

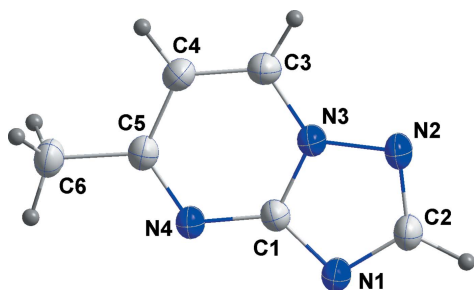


Figure 1
The title molecule with the atom-labelling scheme and 50% probability ellipsoids.

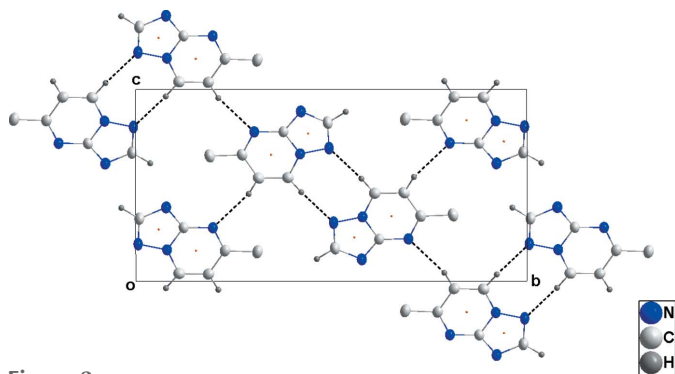


Figure 2
The packing viewed along the *a*-axis direction giving a plan view of the layers. C–H⋯N hydrogen bonds are shown as black dashed lines and the orange dots mark the π–π stacking interactions.

Table 1
Hydrogen-bond geometry (Å, °).

<i>D</i> –H⋯ <i>A</i>	<i>D</i> –H	H⋯ <i>A</i>	<i>D</i> ⋯ <i>A</i>	<i>D</i> –H⋯ <i>A</i>
C2–H2⋯N1 ⁱ	1.016 (17)	2.550 (19)	3.4052 (18)	141.5 (13)
C3–H3⋯N2 ^{vi}	0.979 (18)	2.525 (18)	3.4822 (18)	165.8 (13)
C4–H4⋯N4 ^{viii}	0.946 (19)	2.642 (19)	3.5677 (17)	165.9 (14)

Symmetry codes: (i) $-x + 2, -y + 1, -z + 2$; (vi) $-x, -y + 1, -z + 1$; (viii) $x - 1, -y + \frac{1}{2}, z - \frac{1}{2}$.

4. Hirshfeld surface analysis

In order to visualize the intermolecular interactions in the crystal of the title compound, a Hirshfeld surface (HS) analysis (Hirshfeld, 1977; Spackman & Jayatilaka, 2009) was carried out using *CrystalExplorer17.5* (Turner *et al.*, 2017). In the HS plotted over d_{norm} (Fig. 4), the white surface indicates contacts with distances equal to the sum of the van der Waals

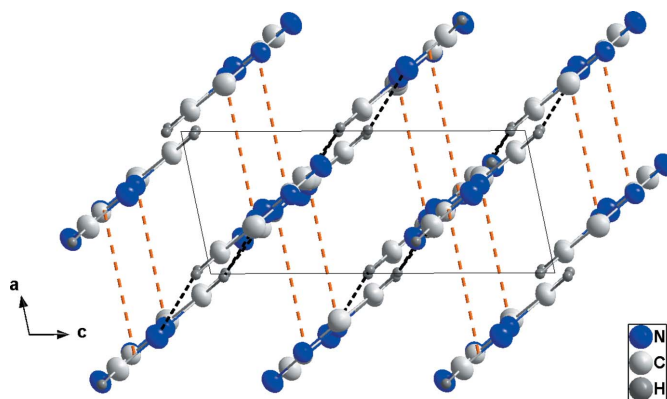


Figure 3
Packing seen along the *b*-axis direction giving a side view of the layers. Hydrogen bonds are depicted as in Fig. 2 and the π–π stacking interactions are shown as orange dashed lines.

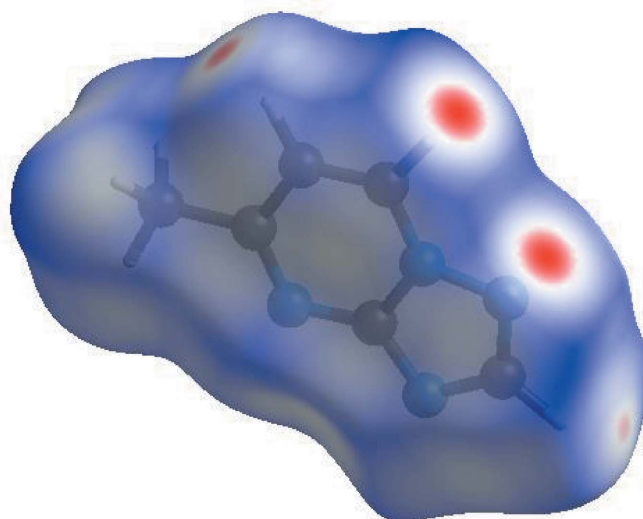
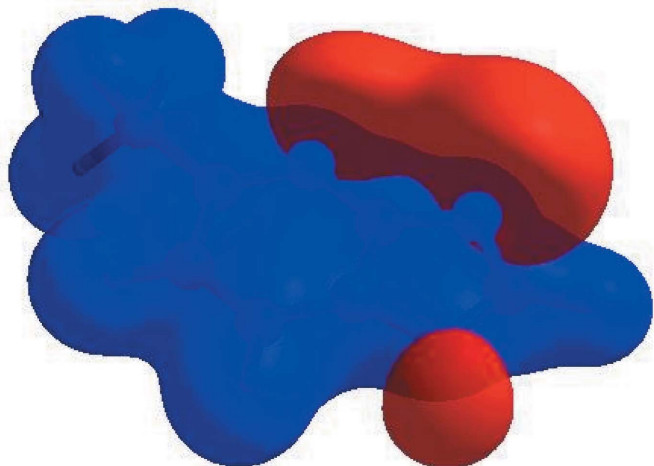
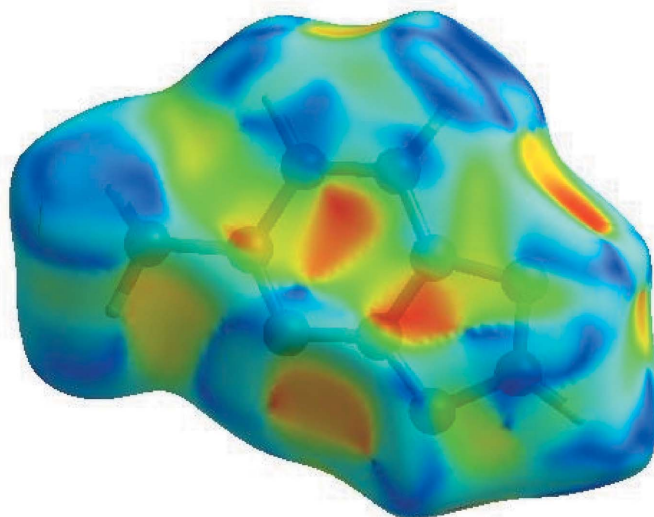


Figure 4
View of the three-dimensional Hirshfeld surface of the title compound plotted over d_{norm} in the range -0.1566 to 1.0057 a.u.


Figure 5

View of the three-dimensional Hirshfeld surface of the title compound plotted over electrostatic potential in the range -0.0500 to 0.0500 a.u. using the STO-3 G basis set at the Hartree–Fock level of theory. Hydrogen-bond donors and acceptors are shown as blue and red regions around the atoms corresponding to positive and negative potentials, respectively.

radii, and the red and blue colours indicate distances shorter (in close contact) or longer (distinct contact), respectively, than the van der Waals radii (Venkatesan *et al.*, 2016). The bright-red spots appearing near N2 and hydrogen atoms H2, H3 and H4 indicate their roles as the respective donors and/or acceptors in the dominant C–H \cdots N hydrogen bonds; they also appear as blue and red regions corresponding to positive and negative potentials on the HS mapped over electrostatic potential (Spackman *et al.*, 2008; Jayatilaka *et al.*, 2005) as shown in Fig. 5. The blue regions indicate positive electrostatic potential (hydrogen-bond donors), while the red regions indicate negative electrostatic potential (hydrogen-bond acceptors). The shape-index of the HS is a tool to visualize π – π stacking by the presence of adjacent red and blue triangles;


Figure 6

Hirshfeld surface of the title compound plotted over shape-index.

Table 2

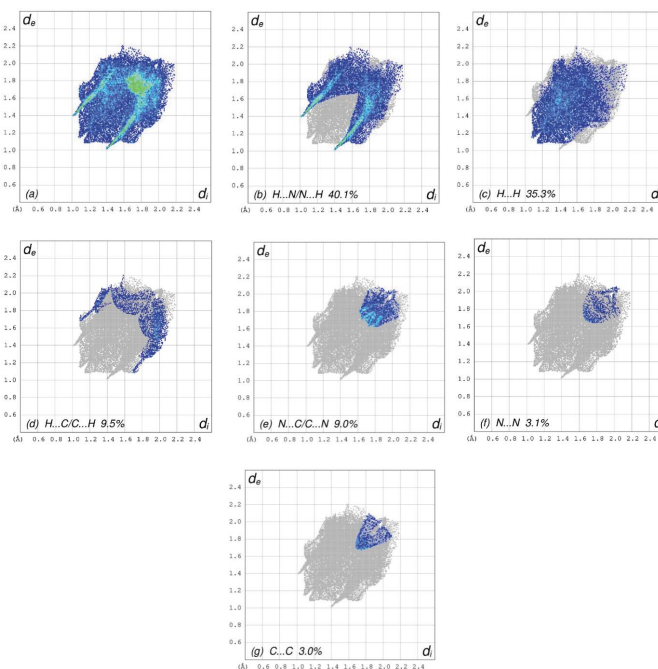
Selected interatomic distances (\AA).

N1 \cdots C2 ⁱ	3.4051 (19)	C1 \cdots C4 ⁱⁱⁱ	3.5667 (19)
N2 \cdots C2 ⁱⁱ	3.385 (2)	C2 \cdots C6 ^{vii}	3.5715 (18)
N3 \cdots C3 ⁱⁱⁱ	3.4163 (19)	C2 \cdots C2 ⁱ	3.595 (2)
N4 \cdots C5 ⁱⁱⁱ	3.4314 (17)	C4 \cdots C5 ⁱⁱ	3.4986 (19)
N4 \cdots C4 ⁱⁱⁱ	3.4177 (19)	C1 \cdots H6B ^{iv}	2.94 (3)
N1 \cdots H6B ^{iv}	2.85 (2)	C6 \cdots H6C ⁱⁱⁱ	2.98 (3)
N1 \cdots H2 ^j	2.553 (18)	H2 \cdots C6 ^{vii}	2.773 (16)
N1 \cdots H6C ^v	2.86 (3)	H2 \cdots H6B ^{vii}	2.58 (3)
N2 \cdots H3 ^{vi}	2.525 (18)	H2 \cdots H6C ^{vii}	2.48 (3)
N4 \cdots H4 ^v	2.641 (18)	H6A \cdots H4 ^v	2.59 (3)
N4 \cdots H6B ^{iv}	2.84 (3)	H6B \cdots H6C ⁱⁱⁱ	2.47 (4)
C1 \cdots C3 ⁱⁱⁱ	3.4166 (19)		

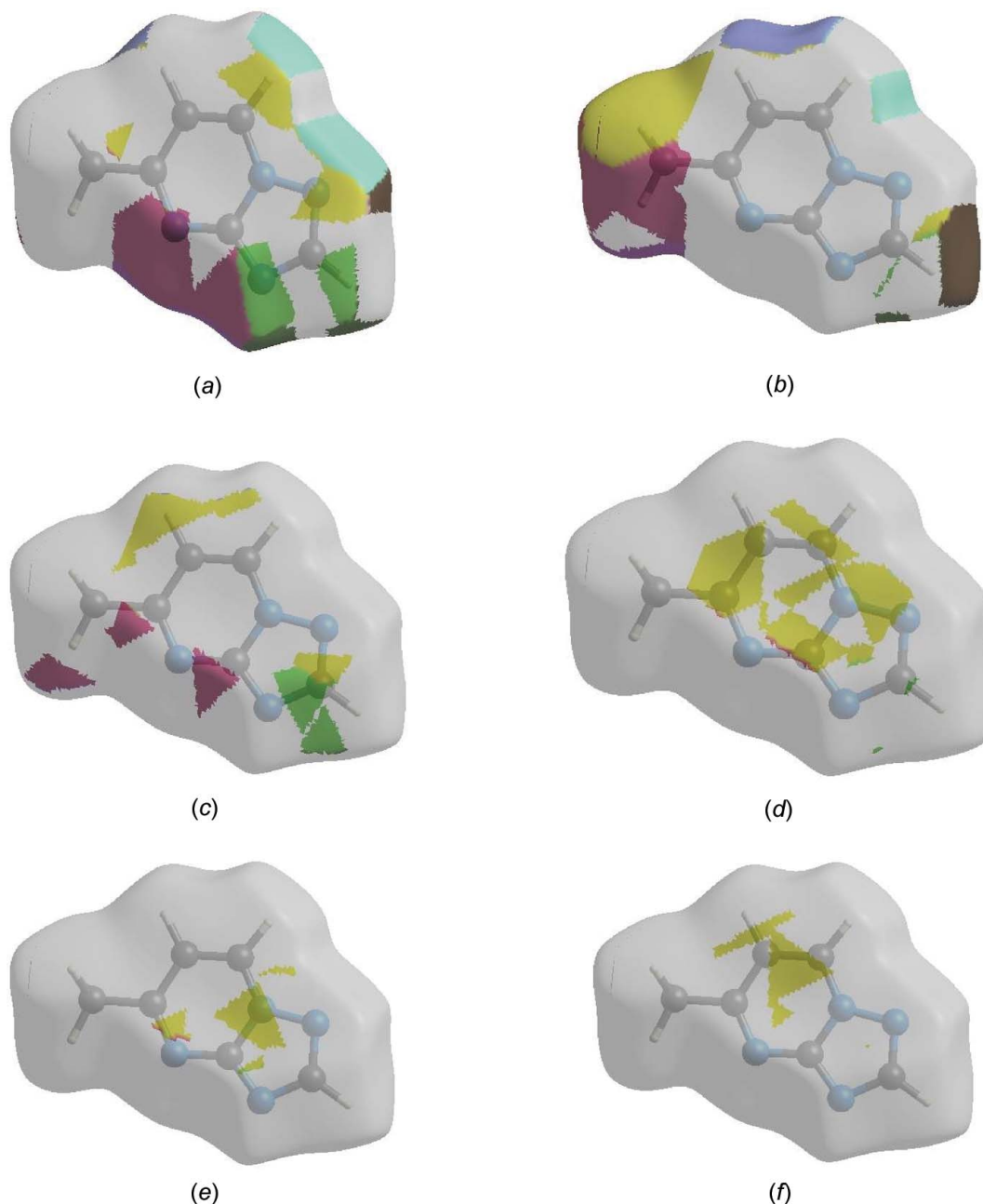
Symmetry codes: (i) $-x+2, -y+1, -z+2$; (ii) $x-1, y, z$; (iii) $x+1, y, z$; (iv) $x, -y+\frac{1}{2}, z+\frac{1}{2}$; (v) $x+1, -y+\frac{1}{2}, z+\frac{1}{2}$; (vi) $-x, -y+1, -z+1$; (vii) $-x+1, y+\frac{1}{2}, -z+\frac{3}{2}$.

if there are no adjacent red and/or blue triangles, then there are no π – π interactions. Fig. 6 clearly suggest that there are π – π interactions present in the crystal structure of (I).

The overall two-dimensional fingerprint plot, Fig. 7(a), and those delineated into H \cdots N/N \cdots H, H \cdots H, H \cdots C/C \cdots H, N \cdots C/C \cdots N, N \cdots N and C \cdots C contacts (McKinnon *et al.*, 2007) are illustrated in Fig. 7(b)–(g), respectively, together with their relative contributions to the Hirshfeld surface. The most important interaction is H \cdots N/N \cdots H, contributing 40.1% to the overall crystal packing, which is reflected in Fig. 7(b) as a pair of characteristic wings with the tips at $d_e + d_i = 2.40$ \AA arising from the C–H \cdots N hydrogen bonds (Table 1) as well as from the H \cdots N/N \cdots H contacts (Table 3). The split


Figure 7

The full two-dimensional fingerprint plots for the title compound, showing (a) all interactions, and delineated into (b) H \cdots N/N \cdots H, (c) H \cdots H, (d) H \cdots C/C \cdots H, (e) N \cdots C/C \cdots N, (f) N \cdots N and (g) C \cdots C interactions. The d_i and d_e values are the closest internal and external distances (in \AA) from given points on the Hirshfeld surface contacts.


Figure 8

The Hirshfeld surface representations with the function d_{norm} plotted onto the surface for (a) $\text{H}\cdots\text{N}/\text{N}\cdots\text{H}$, (b) $\text{H}\cdots\text{H}$, (c) $\text{H}\cdots\text{C}/\text{C}\cdots\text{H}$, (d) $\text{N}\cdots\text{C}/\text{C}\cdots\text{N}$, (e) $\text{N}\cdots\text{N}$ and (f) $\text{C}\cdots\text{C}$ interactions.

thin and thick pair of wings with the tips at $d_e + d_i \sim 2.23 \text{ \AA}$ in Fig. 7(c), arise from the short interatomic $\text{H}\cdots\text{H}$ contacts, which make a 35.3% contribution to the HS and are seen as widely scattered points of high density arising from the large hydrogen content of the molecule. In the absence of $\text{C}-\text{H}\cdots\pi$ interactions, the pair of wings in the fingerprint plot delineated into $\text{H}\cdots\text{C}/\text{C}\cdots\text{H}$ contacts (9.5% contribution to the HS) have a nearly symmetrical distribution of points, Fig. 7(d), with the tips at $d_e + d_i \sim 2.77 \text{ \AA}$. The $\text{N}\cdots\text{C}/\text{C}\cdots\text{N}$ [Fig. 7(e)] and $\text{N}\cdots\text{N}$ [Fig. 7(f)] contacts make contributions of 9.0 and 3.1%, respectively, to the HS and have widely scattered distributions of points. Finally, the $\text{C}\cdots\text{C}$ [Fig. 7(g)] contacts (3.0%

contribution to the HS) have a symmetrical distribution of points, with the tip at $d_e = d_i = 1.69 \text{ \AA}$.

The Hirshfeld surface representations with the function d_{norm} plotted onto the surface are shown for the $\text{H}\cdots\text{N}/\text{N}\cdots\text{H}$, $\text{H}\cdots\text{H}$, $\text{H}\cdots\text{C}/\text{C}\cdots\text{H}$, $\text{N}\cdots\text{C}/\text{C}\cdots\text{N}$, $\text{N}\cdots\text{N}$ and $\text{C}\cdots\text{C}$ interactions in Fig. 8(a)–(f), respectively.

The Hirshfeld surface analysis confirms the importance of H-atom contacts in establishing the packing. The large number of $\text{H}\cdots\text{N}/\text{N}\cdots\text{H}$, $\text{H}\cdots\text{H}$ and $\text{H}\cdots\text{C}/\text{C}\cdots\text{H}$ interactions suggest that van der Waals interactions and hydrogen bonding play the major roles in the crystal packing (Hathwar *et al.*, 2015).

Table 3
Experimental details.

Crystal data	
Chemical formula	C ₆ H ₆ N ₄
<i>M_r</i>	134.15
Crystal system, space group	Monoclinic, <i>P</i> ₂ ₁ / <i>c</i>
Temperature (K)	150
<i>a</i> , <i>b</i> , <i>c</i> (Å)	3.7910 (2), 18.0092 (10), 9.0069 (5)
β (°)	101.704 (2)
<i>V</i> (Å ³)	602.14 (6)
<i>Z</i>	4
Radiation type	Cu <i>K</i> α
μ (mm ⁻¹)	0.82
Crystal size (mm)	0.29 × 0.18 × 0.13
Data collection	
Diffractometer	Bruker D8 VENTURE PHOTON 100 CMOS
Absorption correction	Multi-scan (<i>SADABS</i> ; Krause <i>et al.</i> , 2015)
<i>T_{min}</i> , <i>T_{max}</i>	0.67, 0.90
No. of measured, independent and observed [<i>I</i> > 2 σ (<i>I</i>)] reflections	4567, 1205, 1102
<i>R_{int}</i>	0.074
($\sin \theta/\lambda$) _{max} (Å ⁻¹)	0.626
Refinement	
<i>R</i> [<i>F</i> ² > 2 σ (<i>F</i> ²)], <i>wR</i> (<i>F</i> ²), <i>S</i>	0.044, 0.113, 1.10
No. of reflections	1205
No. of parameters	116
H-atom treatment	All H-atom parameters refined
$\Delta\rho_{\text{max}}$, $\Delta\rho_{\text{min}}$ (e Å ⁻³)	0.20, -0.20

Computer programs: *APEX3* and *SAINT* (Bruker, 2016), *SHELXT* (Sheldrick, 2015a), *SHELXL2018* (Sheldrick, 2015b), *DIAMOND* (Brandenburg & Putz, 2012) and *SHELXTL* (Sheldrick, 2008).

5. Database survey

Two structures have previously been reported in which the title compound, (I), is present as a ligand (*L*), namely [Fe(*L*)₂(SCN)₂(H₂O)₂] (Bigini Cingi *et al.*, 1986) and [Cu(μ -*L*)₂(SCN)]_{*n*} (Cornelissen *et al.*, 1989), but to the best of our knowledge, the molecule itself has not previously been structurally characterized.

6. Synthesis and crystallization

To a solution of ethyl-2-[5-methyl-1-[1,2,4]triazolo[1,5-*a*]pyrimidin-7-yl]acetate (1.00 g, 4.5 mmol) in DMF (25 ml) was added 2 eq of bis(2-chloroethyl)amine hydrochloride (1.61 g, 9 mmol), potassium carbonate (1.37 g, 9.9 mmol) and a catalytic amount of tetra-*n*-butylammonium bromide. The mixture was stirred at 353.15 K for 24 h. The solution was filtered and the solvent was removed under reduced pressure. The residue obtained was dissolved in dichloromethane and purified by column chromatography (EtOAc/Hexane, 1:9 *v:v*). The title compound was obtained as colourless crystals in 40% yield.

7. Refinement

Crystal data, data collection and structure refinement details are summarized in Table 2. H atoms were located in a difference Fourier map and were freely refined.

Funding information

The support of NSF–MRI grant No. 1228232 for the purchase of the diffractometer and Tulane University for support of the Tulane Crystallography Laboratory are gratefully acknowledged. TH is grateful to the Hacettepe University Scientific Research Project Unit (grant No. 013 D04 602 004).

References

- Ashour, H., Shaaban, O., Rizk, O. & El-Ashmawy, I. M. (2013). *Eur. J. Med. Chem.* **62**, 341–351.
- Beck, H. P., DeGraffenreid, M., Fox, B., Allen, J. G., Rew, Y., Schneider, S., Saiki, A. Y., Yu, D., Oliner, J. D., Salyers, K., Ye, Q. & Olson, S. (2011). *Bioorg. Med. Chem. Lett.* **21**, 2752–2755.
- Biagini Cingi, M., Manotti Lanfredi, A. M., Tiripicchio, A., Cornelissen, J. P., Haasnoot, J. G. & Reedijk, J. (1986). *Acta Cryst. C* **42**, 1296–1298.
- Brandenburg, K. & Putz, H. (2012). *DIAMOND*, Crystal Impact GbR, Bonn, Germany.
- Bruker (2016). *APEX3* and *SAINT*. Bruker AXS Inc., Madison, Wisconsin, USA.
- Chebanov, V. A., Gura, K. A. & Desenko, S. M. (2010). *Top. Heterocycl. Chem.* **23**, 41–84.
- Cornelissen, J. P., De Graaff, R. A. G., Haasnoot, J. G., Prins, R., Reedijk, J., Biagini-Cingi, M., Manotti-Lanfredi, A. M. & Tiripicchio, A. (1989). *Polyhedron*, **8**, 2313–2320.
- Hathwar, V. R., Sist, M., Jørgensen, M. R. V., Mamakhel, A. H., Wang, X., Hoffmann, C. M., Sugimoto, K., Overgaard, J. & Iversen, B. B. (2015). *IUCrJ*, **2**, 563–574.
- Hirshfeld, H. L. (1977). *Theor. Chim. Acta*, **44**, 129–138.
- Hoffmann, K., Wiśniewska, J., Wojtczak, A., Sitkowski, J., Denslow, A., Wietrzyk, J., Jakubowski, M. & Łakomska, I. (2017). *J. Inorg. Biochem.* **172**, 34–45.
- Jayatilaka, D., Grimwood, D. J., Lee, A., Lemay, A., Russel, A. J., Taylor, C., Wolff, S. K., Cassam-Chenai, P. & Whitton, A. (2005). *TONTO - A System for Computational Chemistry*. Available at: <http://hirshfeldsurface.net/>
- Krause, L., Herbst-Irmer, R., Sheldrick, G. M. & Stalke, D. (2015). *J. Appl. Cryst.* **48**, 3–10.
- Lahmidi, S., El Hafi, M., Moussaif, A., Benchidmi, M., Essassi, E. M. & Mague, J. T. (2018). *IUCrData*, **3**, x181280.
- Lahmidi, S., Sebbar, N. K., Boulhaoua, M., Essassi, E. M., Mague, J. T. & Zouihri, H. (2016a). *IUCrData*, **1**, x160870.
- Lahmidi, S., Sebbar, N. K., Harmaoui, A., Ouzidan, Y., Essassi, E. M. & Mague, J. T. (2016b). *IUCrData*, **1**, x161946.
- Mabkhot, Y. N., Alatibi, F., El-Sayed, N. N. E., Kheder, N. A. & Al-Showiman, S. (2016). *Molecules*, **21**, 1036–1045.
- McKinnon, J. J., Jayatilaka, D. & Spackman, M. A. (2007). *Chem. Commun.* pp. 3814.
- Sedash, Y. V., Gorobets, N. Y., Chebanov, V. A., Konvalova, I. S., Shishkin, O. V. & Desenko, S. M. (2012). *RSC Adv.* **2**, 6719–6728.
- Sheldrick, G. M. (2008). *Acta Cryst.* **A64**, 112–122.
- Sheldrick, G. M. (2015a). *Acta Cryst.* **A71**, 3–8.
- Sheldrick, G. M. (2015b). *Acta Cryst.* **C71**, 3–8.
- Spackman, M. A. & Jayatilaka, D. (2009). *CrystEngComm*, **11**, 19–32.
- Spackman, M. A., McKinnon, J. J. & Jayatilaka, D. (2008). *CrystEngComm*, **10**, 377–388.
- Turner, M. J., McKinnon, J. J., Wolff, S. K., Grimwood, D. J., Spackman, P. R., Jayatilaka, D. & Spackman, M. A. (2017). *CrystalExplorer17*. The University of Western Australia.
- Venkatesan, P., Thamotharan, S., Ilangovan, A., Liang, H. & Sundius, T. (2016). *Spectrochim. Acta Part A*, **153**, 625–636.

supporting information

Acta Cryst. (2018). E74, 1833-1837 [https://doi.org/10.1107/S2056989018016225]

Crystal structure and Hirshfeld surface analysis of 5-methyl-1,2,4-triazolo[1,5-a]pyrimidine

Sanae Lahmidi, Nada Kheira Sebbar, Tuncer Hökelek, Karim Chkirate, Joel T. Mague and El Mokhtar Essassi

Computing details

Data collection: *APEX3* (Bruker, 2016); cell refinement: *S SAINT* (Bruker, 2016); data reduction: *S SAINT* (Bruker, 2016); program(s) used to solve structure: *SHELXT* (Sheldrick, 2015a); program(s) used to refine structure: *SHELXL2018* (Sheldrick, 2015b); molecular graphics: *DIAMOND* (Brandenburg & Putz, 2012); software used to prepare material for publication: *SHELXTL* (Sheldrick, 2008).

5-Methyl-1,2,4-triazolo[1,5-a]pyrimidine

Crystal data

$C_6H_6N_4$

$M_r = 134.15$

Monoclinic, $P2_1/c$

$a = 3.7910$ (2) Å

$b = 18.0092$ (10) Å

$c = 9.0069$ (5) Å

$\beta = 101.704$ (2)°

$V = 602.14$ (6) Å³

$Z = 4$

$F(000) = 280$

$D_x = 1.480$ Mg m⁻³

Cu $K\alpha$ radiation, $\lambda = 1.54178$ Å

Cell parameters from 3969 reflections

$\theta = 4.9\text{--}74.7^\circ$

$\mu = 0.82$ mm⁻¹

$T = 150$ K

Column, colourless

$0.29 \times 0.18 \times 0.13$ mm

Data collection

Bruker D8 VENTURE PHOTON 100 CMOS diffractometer

Radiation source: INCOATEC $I\mu$ S micro-focus source

Mirror monochromator

Detector resolution: 10.4167 pixels mm⁻¹

ω scans

Absorption correction: multi-scan (*SADABS*; Krause *et al.*, 2015)

$T_{\min} = 0.67$, $T_{\max} = 0.90$

4567 measured reflections

1205 independent reflections

1102 reflections with $I > 2\sigma(I)$

$R_{\text{int}} = 0.074$

$\theta_{\max} = 74.7^\circ$, $\theta_{\min} = 4.9^\circ$

$h = -4 \rightarrow 4$

$k = -22 \rightarrow 21$

$l = -11 \rightarrow 10$

Refinement

Refinement on F^2

Least-squares matrix: full

$R[F^2 > 2\sigma(F^2)] = 0.044$

$wR(F^2) = 0.113$

$S = 1.10$

1205 reflections

116 parameters

0 restraints

Primary atom site location: structure-invariant direct methods

Secondary atom site location: difference Fourier map

Hydrogen site location: difference Fourier map

All H-atom parameters refined

$w = 1/[\sigma^2(F_o^2) + (0.0458P)^2 + 0.1643P]$

where $P = (F_o^2 + 2F_c^2)/3$

$$(\Delta/\sigma)_{\max} < 0.001$$

$$\Delta\rho_{\max} = 0.20 \text{ e } \text{\AA}^{-3}$$

$$\Delta\rho_{\min} = -0.20 \text{ e } \text{\AA}^{-3}$$

Extinction correction: *SHELXL2018* (Sheldrick, 2015b), $F_c^* = kFc[1 + 0.001xFc^2\lambda^3/\sin(2\theta)]^{-1/4}$
 Extinction coefficient: 0.021 (4)

Special details

Geometry. All esds (except the esd in the dihedral angle between two l.s. planes) are estimated using the full covariance matrix. The cell esds are taken into account individually in the estimation of esds in distances, angles and torsion angles; correlations between esds in cell parameters are only used when they are defined by crystal symmetry. An approximate (isotropic) treatment of cell esds is used for estimating esds involving l.s. planes.

Refinement. Refinement of F^2 against ALL reflections. The weighted R-factor wR and goodness of fit S are based on F^2 , conventional R-factors R are based on F, with F set to zero for negative F^2 . The threshold expression of $F^2 > 2\sigma(F^2)$ is used only for calculating R-factors(gt) etc. and is not relevant to the choice of reflections for refinement. R-factors based on F^2 are statistically about twice as large as those based on F, and R-factors based on ALL data will be even larger.

Fractional atomic coordinates and isotropic or equivalent isotropic displacement parameters (\AA^2)

	x	y	z	$U_{\text{iso}}^*/U_{\text{eq}}$
N1	0.7561 (3)	0.42236 (6)	0.88570 (13)	0.0322 (3)
N2	0.4407 (3)	0.49411 (6)	0.69436 (15)	0.0341 (3)
N3	0.3764 (3)	0.42019 (6)	0.66430 (13)	0.0281 (3)
N4	0.5532 (3)	0.30294 (6)	0.77958 (13)	0.0277 (3)
C1	0.5676 (3)	0.37780 (7)	0.78059 (15)	0.0269 (3)
C2	0.6678 (4)	0.49082 (7)	0.82759 (17)	0.0340 (4)
H2	0.776 (5)	0.5371 (9)	0.883 (2)	0.037 (4)*
C3	0.1587 (4)	0.38918 (7)	0.54119 (15)	0.0313 (3)
H3	0.025 (5)	0.4230 (9)	0.465 (2)	0.037 (4)*
C4	0.1409 (4)	0.31397 (7)	0.53851 (16)	0.0302 (3)
H4	-0.006 (5)	0.2889 (10)	0.456 (2)	0.039 (4)*
C5	0.3442 (3)	0.27179 (7)	0.66009 (15)	0.0279 (3)
C6	0.3279 (4)	0.18893 (7)	0.65408 (19)	0.0344 (4)
H6A	0.462 (6)	0.1656 (13)	0.749 (3)	0.066 (6)*
H6B	0.431 (6)	0.1705 (12)	0.576 (3)	0.071 (7)*
H6C	0.095 (7)	0.1716 (12)	0.629 (3)	0.073 (7)*

Atomic displacement parameters (\AA^2)

	U^{11}	U^{22}	U^{33}	U^{12}	U^{13}	U^{23}
N1	0.0381 (6)	0.0233 (5)	0.0321 (6)	-0.0020 (4)	0.0000 (5)	-0.0010 (4)
N2	0.0434 (7)	0.0197 (5)	0.0367 (6)	-0.0011 (4)	0.0026 (5)	0.0000 (4)
N3	0.0324 (6)	0.0222 (5)	0.0281 (6)	-0.0001 (4)	0.0024 (5)	0.0005 (4)
N4	0.0311 (6)	0.0221 (5)	0.0289 (6)	-0.0004 (4)	0.0040 (5)	-0.0003 (4)
C1	0.0297 (6)	0.0224 (6)	0.0280 (7)	0.0001 (4)	0.0041 (5)	0.0011 (4)
C2	0.0414 (8)	0.0221 (6)	0.0360 (8)	-0.0023 (5)	0.0020 (6)	-0.0019 (5)
C3	0.0337 (7)	0.0304 (7)	0.0281 (7)	0.0005 (5)	0.0020 (5)	0.0005 (5)
C4	0.0319 (7)	0.0289 (7)	0.0284 (7)	-0.0030 (5)	0.0026 (5)	-0.0029 (5)
C5	0.0284 (6)	0.0250 (6)	0.0308 (7)	-0.0016 (5)	0.0074 (5)	-0.0022 (5)
C6	0.0386 (8)	0.0244 (7)	0.0393 (8)	-0.0022 (5)	0.0058 (7)	-0.0043 (5)

Geometric parameters (Å, °)

N1—C1	1.3329 (17)	C3—C4	1.3560 (18)
N1—C2	1.3545 (17)	C3—H3	0.979 (18)
N2—C2	1.329 (2)	C4—C5	1.4241 (19)
N2—N3	1.3703 (15)	C4—H4	0.946 (19)
N3—C3	1.3607 (17)	C5—C6	1.4940 (18)
N3—C1	1.3775 (17)	C6—H6A	1.00 (2)
N4—C5	1.3245 (17)	C6—H6B	0.94 (3)
N4—C1	1.3492 (17)	C6—H6C	0.92 (3)
C2—H2	1.016 (17)		
N1...C2 ⁱ	3.4051 (19)	C1...C4 ⁱⁱⁱ	3.5667 (19)
N2...C2 ⁱⁱ	3.385 (2)	C2...C6 ^{vii}	3.5715 (18)
N3...C3 ⁱⁱⁱ	3.4163 (19)	C2...C2 ⁱ	3.595 (2)
N4...C5 ⁱⁱⁱ	3.4314 (17)	C4...C5 ⁱⁱ	3.4986 (19)
N4...C4 ⁱⁱⁱ	3.4177 (19)	C1...H6B ^{iv}	2.94 (3)
N1...H6B ^{iv}	2.85 (2)	C6...H6C ⁱⁱⁱ	2.98 (3)
N1...H2 ⁱ	2.553 (18)	H2...C6 ^{vii}	2.773 (16)
N1...H6C ^v	2.86 (3)	H2...H6B ^{vii}	2.58 (3)
N2...H3 ^{vi}	2.525 (18)	H2...H6C ^{vii}	2.48 (3)
N4...H4 ^v	2.641 (18)	H6A...H4 ^v	2.59 (3)
N4...H6B ^{iv}	2.84 (3)	H6B...H6C ⁱⁱⁱ	2.47 (4)
C1...C3 ⁱⁱⁱ	3.4166 (19)		
C1—N1—C2	102.64 (11)	N3—C3—H3	117.3 (10)
C2—N2—N3	101.05 (10)	C3—C4—C5	120.13 (12)
C3—N3—N2	127.88 (11)	C3—C4—H4	120.6 (11)
C3—N3—C1	122.05 (11)	C5—C4—H4	119.3 (11)
N2—N3—C1	110.07 (11)	N4—C5—C4	122.68 (12)
C5—N4—C1	116.45 (11)	N4—C5—C6	117.78 (12)
N1—C1—N4	128.43 (12)	C4—C5—C6	119.54 (12)
N1—C1—N3	109.26 (11)	C5—C6—H6A	112.4 (14)
N4—C1—N3	122.30 (12)	C5—C6—H6B	111.1 (13)
N2—C2—N1	116.97 (12)	H6A—C6—H6B	106.4 (19)
N2—C2—H2	122.2 (10)	C5—C6—H6C	112.2 (14)
N1—C2—H2	120.8 (10)	H6A—C6—H6C	111.5 (19)
C4—C3—N3	116.38 (12)	H6B—C6—H6C	103 (2)
C4—C3—H3	126.3 (10)		
C2—N2—N3—C3	179.68 (13)	N3—N2—C2—N1	0.14 (17)
C2—N2—N3—C1	0.03 (14)	C1—N1—C2—N2	-0.24 (17)
C2—N1—C1—N4	179.97 (13)	N2—N3—C3—C4	-179.91 (12)
C2—N1—C1—N3	0.24 (14)	C1—N3—C3—C4	-0.30 (18)
C5—N4—C1—N1	-179.67 (12)	N3—C3—C4—C5	-0.18 (19)
C5—N4—C1—N3	0.04 (17)	C1—N4—C5—C4	-0.53 (17)
C3—N3—C1—N1	-179.85 (12)	C1—N4—C5—C6	178.84 (11)
N2—N3—C1—N1	-0.18 (14)	C3—C4—C5—N4	0.6 (2)

C3—N3—C1—N4	0.39 (18)	C3—C4—C5—C6	-178.74 (13)
N2—N3—C1—N4	-179.93 (11)		

Symmetry codes: (i) $-x+2, -y+1, -z+2$; (ii) $x-1, y, z$; (iii) $x+1, y, z$; (iv) $x, -y+1/2, z+1/2$; (v) $x+1, -y+1/2, z+1/2$; (vi) $-x, -y+1, -z+1$; (vii) $-x+1, y+1/2, -z+3/2$.

Hydrogen-bond geometry (Å, °)

<i>D—H...A</i>	<i>D—H</i>	<i>H...A</i>	<i>D...A</i>	<i>D—H...A</i>
C2—H2...N1 ⁱ	1.016 (17)	2.550 (19)	3.4052 (18)	141.5 (13)
C3—H3...N2 ^{vi}	0.979 (18)	2.525 (18)	3.4822 (18)	165.8 (13)
C4—H4...N4 ^{viii}	0.946 (19)	2.642 (19)	3.5677 (17)	165.9 (14)

Symmetry codes: (i) $-x+2, -y+1, -z+2$; (vi) $-x, -y+1, -z+1$; (viii) $x-1, -y+1/2, z-1/2$.